

Super-resolution fluorescence microscopy for investigating bacterial macromolecular complexes

Alexander Carsten¹, Manuel Wolters¹, and Martin Aepfelbacher¹

¹Universitätsklinikum Hamburg-Eppendorf Institut für Medizinische Mikrobiologie Virologie und Hygiene

August 5, 2023

Abstract

Super-resolution fluorescence microscopy techniques developed over the past two decades have pushed the resolution limit for fluorescently labeled molecules into the nanometer range. These techniques have the potential to study bacterial macromolecular complexes such as secretion systems with single-molecule resolution on a millisecond time scale. Here we review recent applications of super-resolution fluorescence microscopy in molecular bacteriology with a focus on bacterial secretion systems. We also describe MINFLUX fluorescence nanoscopy, a relatively new technique that promises to one day produce molecular movies of bacterial molecular machines in action.

Introduction

The dimensions of most bacterial cells are in the micrometer range and thus come close to the diffraction limit of visible light of about 200-300 nm (Fig. 1A). Therefore, to resolve the details and dynamics of crucial bacterial activities, novel techniques are necessary. Recent developments in fluorescence super-resolution microscopy (SRM) are promising to move closer to the goal of observing the localization and motion of single proteins in living bacterial cells. SRM techniques have the potential to revolutionize the understanding of central processes in bacteria e.g., peptidoglycan assembly, the mode of action of DNA-binding proteins, the function of macromolecular machines involved in protein secretion, DNA replication or antibiotic resistance. In this review, we describe recent work showing the importance of fluorescence SRM for understanding complex molecular structures and functions in bacteria. Special attention will be paid to the MINFLUX nanoscopy technique, which is a promising approach to visualize the molecular motions and dynamic interactions of single molecules with a spatiotemporal resolution in the single-digit nanometer and low millisecond range. Applications of SRM methods including MINFLUX nanoscopy to observe individual components of a molecular machine, the bacterial type 3 secretion system (T3SS), will be described in more detail. While the focus of this review is on the visualization of molecular processes in bacteria, all of the described microscopy approaches are also applied in other cell types. A widely applicable workflow guiding researchers towards *in cellulo* MINFLUX imaging at molecular scale has been described previously (Carsten et al., 2022).

Fluorescence super-resolution microscopy techniques

Fluorescence SRM techniques can achieve resolutions and localization precisions far below the diffraction limit of light of about 200-300 nm. Among them, structured illumination microscopy (SIM) is a wide field approach that illuminates the sample with a periodical (most of the time sinusoidal patterned) excitation light. While the excitation pattern is shifted and turned with respect to the sample, multiple pictures need to be acquired. Fourier transformation-based algorithms are applied on the acquired frames to produce the final image (Gustafsson, 2000). Linear SIM can improve the lateral resolution to about 120 nm and the axial resolution to about 300 nm (Gustafsson et al., 2008). Linear SIM has been used widely in bacterial cell

biology and e.g., allowed an improved visualization of different secretion systems (Nauth et al., 2018, Lin et al., 2022).

Two fluorescence microscopy technologies achieving resolutions down to about 20-30 nm have been particularly successful in imaging diverse biological systems. These are on the one hand laser-scanning based super-resolution approaches like stimulated emission depletion (STED) nanoscopy, which directly records super-resolved images (Hell and Wichmann, 1994, Klar and Hell, 1999) and, on the other hand, wide field based single molecule localization microscopy (SMLM) approaches including (direct) stochastic optical reconstruction microscopy ((d)STORM), photoactivated localization microscopy (PALM) and points accumulation for imaging in nanoscale topography (PAINT). Here, fluorescent emissions of single fluorophores are localized below the diffraction limit over time (Betzig et al., 2006, Rust et al., 2006, Schnitzbauer et al., 2017).

Recently, minimal photon flux (MINFLUX) nanoscopy has been shown to reach resolutions and localization precisions down to 1 nm. MINFLUX nanoscopy is a laser scanning SMLM technique that combines features of STED nanoscopy and SMLM. The precise localization of single fluorophores is achieved by determining their position with respect to the centre of a donut-shaped excitation beam that is scanned through the sample. Moving the excitation beam with an excitation minimum at its center around the target molecule in order to find the minimum excitation point, MINFLUX nanoscopy enables localization of fluorophores using a minimal number of photons (Balzarotti et al., 2017, Schmidt et al., 2021).

An entirely different but still worth mentioning approach to visualize sub-diffraction limited details in biological samples is Expansion Microscopy. Here, the biological samples (e.g., tissues, cells, bacterial infection models) are expanded isotropically with help of a swellable polymer matrix thus physically enlarging the biological structures by a factor of 4.5 to 10, which results in an increased (pseudo-) resolution independent of the microscopy technique used (Truckenbrodt et al., 2018, Chen et al., 2015). Presently there are only a few published studies in which Expansion Microscopy has been used in bacteria (i.e. (Kunz et al., 2021, Gotz et al., 2020)). It needs to be carefully evaluated whether individual components of structures of interest, e.g., secretion systems, are expanded with the same factor in all dimensions (Buttner et al., 2021).

A key role for performing successful super-resolution microscopy in microbiology is played by the sample preparation with respect to the fluorescent labels that are available. For fluorescence microscopy in biological specimens, the molecules of interest must be marked with a fluorescent probe. If a tag is introduced into the endogenously- or heterologously expressed molecule of interest, care must be taken to ensure that the tag does not interfere with the function of the molecule. Also, overexpression of heterologous molecules can produce artifacts in biological samples (Bolognesi and Lehner, 2018). Another aspect to consider, especially when using super-resolution microscopy techniques, is that the fluorescent label must be positioned as close as possible to the molecule of interest to take full advantage of the achievable single-digit nanometer resolution. For example, a combination of primary and fluorescently labeled secondary antibodies can already offset the fluorescent label by up to 20 nm relative to the molecule of interest (Fruh et al., 2021). To minimize the label error, fluorescent proteins, self-labeling enzyme (SLE) tags (SNAP, Halo, CLIP) and nanobodies of around 3 nm in size have successfully been employed (Liss et al., 2015, Ries et al., 2012, Carsten et al., 2022, Banaz et al., 2019) (Fig. 1B). The label error in the visualization of proteins can also be reduced to the subnanometer scale by introducing noncanonical amino acids with bioorthogonal (“clickable”) side chains (Mihaila et al., 2022). An overview and more detailed information on labeling approaches and fluorescent probes suitable for super-resolution fluorescence microscopy have been published elsewhere (Liu et al., 2022).

Super-resolution fluorescence microscopy in bacterial cell biology

Deciphering the precise timing and localization of peptidoglycan synthesis in Gram-negative and Gram-positive bacteria is a long-standing goal in molecular bacteriology and may be of medical importance, for example, in the development of new antibiotics. In one study, fluorescent D-amino acids were incorporated into bacterial peptidoglycans and imaged by STED nanoscopy at below 100 nm resolution (Soderstrom et al., 2020). In another study, bioorthogonal metabolic labeling of peptidoglycan in *Streptococcus pneumoniae* was successfully combined with dSTORM (Trouve et al., 2021). Cephalosporin-, metabolic- and hydroxylamine-

based fluorescent probes in combination with d-STORM revealed the molecular details of how peptidoglycan dynamics in *Staphylococcus aureus* are controlled during growth and division (Lund et al., 2022). 3D-SIM demonstrated that SepF transiently co-localizes with FtsZ at the septum of the archaeon *Methanobrevibacter smithii*. It was found that SepF is the relevant FtsZ anchor and possibly primes the future division plane (Pende et al., 2021). Combinations of STORM or SIM super-resolution fluorescence microscopy with atomic force microscopy (AFM), named STORMForce or SIMForce respectively, revealed the intricate spatiotemporal 3D dynamics of peptidoglycan synthesis during growth and division in *Bacillus subtilis* (Tank et al., 2021). 3D-SIM helped identify the molecular function and interaction partners of a *Helicobacter pylori* bactofilin (CcmA), that plays a crucial role in generating the distinctive helical shape of the bacteria. CcmA aids coordinate cell shape-determining proteins and peptidoglycan synthesis machinery to organize cell wall synthesis and curvature (Sichel et al., 2022). SIM of fluorescently labeled teixobactin, a recently introduced antibiotic, allowed visualization of teixobactin interactions and structural organization in the Gram-positive cell wall. This provided insights into the mechanism of action of teixobactin and could contribute to the development of antibiotics with similar properties (Morris et al., 2022). PALM and dSTORM were employed to study the subcellular localization of proteins at the surface and in the cytoplasm of *Mycoplasma* spp., which are the smallest known bacteria with sizes of 300 to 800 nm. Because of their tiny genomes and sizes, these human and animal pathogens represent important model organisms for synthetic biology, and super-resolution microscopy techniques will greatly improve the understanding of their biology (Rideau et al., 2022). *S. aureus* fibronectin binding receptor organization and adhesion to patches of fibronectin of systematically varied size (100-1000 nm) was investigated using DNA-PAINT. The results suggest that for strong adhesion of *S. aureus* fibronectin patches of 300 nm or larger and the involvement of two or more receptors are required (Khateb et al., 2022). Different SRM and single-molecule tracking (SMT) techniques have been employed to visualize activities of bacterial RNA-polymerases, DNA-binding proteins, the exact spatial organization of DNA replication and transcription, and DNA repair processes in real time (Cassaro and Uphoff, 2022, Uphoff et al., 2013, Stracy et al., 2015). DNA methyltransferases (MTases) have central functions in restriction modification systems, cell cycle regulation, and the control of gene expression. SMLM and SMT of the MTase DnmA revealed its preferential localization to the nucleoid and the replisome region as well as its intracellular dynamics (Fernandez et al., 2023). Single-molecule localization microscopy in *E. coli* cells was employed to investigate enrichment of the translesion synthesis polymerase Pol IV at stalled replication forks in the presence of DNA damage. It turned out that alterations in the dynamics of single-stranded DNA-binding proteins at the replication fork likely contribute to the Pol IV enrichment (Thrall et al., 2022). Microbial biofilms play an important role in both, human infections and biotechnological processes. SR-SIM revealed the distribution of extracellular polysaccharides and DNA in resident biofilms (Wang et al., 2022). The production of extracellular vesicles (EVs) by Gram-positive bacteria was investigated by STORM. The results showed that EV can be formed by membrane blebbing and explosive cell lysis, suggesting that cell wall degradation plays a significant role in their biogenesis (Jeong et al., 2022). Listeriolysin S (LLS) a thiazole/oxazole-modified microcin from *Listeria monocytogenes* was localized to the bacterial cell membrane and cytoplasm using PAINT/dSTORM. This contributed to the understanding of LLS as a contact-dependent bacteriocin (Meza-Torres et al., 2021).

Super-resolution in secretion systems:

Pathogenic bacteria have developed different types of systems to secrete molecules into the extracellular space or to translocate them into host cells (Filloux, 2022). The secreted or translocated molecules often serve as virulence factors, for example, to compete with other bacterial species, to invade mammalian host cells or to evade the host immune system (Galan, 2009, Le et al., 2021). Bacterial secretion systems can consist of a single protein or more than 20 different proteins that combine to form complex macromolecular machines, as in the case of the T3SS (Wagner et al., 2018, Jenkins et al., 2022). Most of our knowledge about the structure and function of secretion systems comes from genetic, biochemical and structural biological as well as electron microscopic studies (Berger et al., 2021, Hu et al., 2018, Lunelli et al., 2020, Marlovits et al., 2004, Worrall et al., 2016).

T3SSs, also called injectisomes, are found in numerous pathogens including *Yersinia*, *Pseudomonas*, *Shigella*

and *Salmonella*, and translocate effector proteins into eukaryotic host cells (Wagner et al., 2018). Although the T3SSs of the various pathogens are highly conserved, the effectors injected by them differ significantly in structure and function and can manipulate a variety of cellular processes. This ultimately determines the interaction of each pathogen with the host and the outcome of the infection (Galan, 2009). T3SSs have a width of 40 nm and a length of 150 nm and consist of both, stable components (needle complex, export apparatus) and transiently associated components (sorting platform, tip complex, pore complex) (Fig. 1A). The needle complex is a multi-ringed cylindrical structure embedded in the bacterial cell envelope and connected to a 30-70 nm long needle filament that points into the extracellular space. Together with the export apparatus, it forms a channel through which the structural and effector proteins of the system are transported (Miletic et al., 2021). At the distal end of the needle is the tip complex, which is involved in host cell recognition, activation of secretion, and regulation of the assembly of the pore complex upon host cell contact (Veenendaal et al., 2007, Deane et al., 2006). Lastly, several cytoplasmic proteins form a heteromultimeric complex known as the sorting platform, which is involved in the selection and sorting of proteins destined for secretion and translocation (Lara-Tejero et al., 2011).

Even though the complexity and presumed molecular dynamics of bacterial secretion systems asks for an investigation with fluorescence microscopic methods, the resolution of these methods has long been insufficient for this purpose. However, novel super-resolution microscopy techniques developed in the last two decades pushed the resolution limit for fluorescently labeled molecules into the nanometer range (Fig. 1A). Such techniques now also allow the study of bacterial secretion systems at much higher resolution (Sahl et al., 2017). Some relevant reports on this subject are presented below.

In an early systematic analysis, the suitability of the SLEs HaloTag and SNAP-tag for super resolution microscopy of different *Salmonella enterica* secretion system subunits was tested. The tags were genetically linked to subunits of a type I secretion system (T1SS) and T3SS (and to the flagellar rotor and a transcription factor), the tagged proteins were labeled by cell-permeable dyes and analyzed by dSTORM and SMT. This allowed determination of the number, subcellular localization and dynamics of protein complexes in living bacteria (Barlag et al., 2016). In a follow-up study, *S. enterica* T3SS effectors fused to SLEs were found to be translocated into host cells where they remained functional and were properly located (Goser et al., 2019). However, it is important to consider that the SLEs may be secreted with greatly varying efficiency depending on the type of tagged protein and T3SS involved species (Singh and Kenney, 2021).

Using PALM, the intrabacterial distribution of the ATPase SecA, which is the driving force for protein secretion by the SecYEG translocon, was evaluated in *E. coli*. SecA was mostly localized as a homodimer along the cytoplasmic membrane and diffused along it in three different diffusion rate populations as found by SMT (Seinen et al., 2021).

The type I secretion system substrate hemolysin A (HlyA) was imaged on the surface of *E. coli* using SIM. In contrast to other bacterial secretion systems, HlyA showed no polarization on the cell surface and its distribution was not influenced by cell growth and division cycle (Beer et al., 2022).

Using SIM, the sfGFP-labeled inner membrane component VirB6 of the *Agrobacterium tumefaciens* type 4 secretion system was found to preferentially localize to the cell poles (Mary et al., 2018). SIM was also employed to subcellularly localize type 6 secretion system (T6SS) assembly in response to cell-cell contact in *Acinetobacter baylyi*, *Acinetobacter baumannii* and *Burkholderia thailandensis*. Employing sfGFP-tagged sheath protein TssB, the polymerization rate and time as well as the disassembly of the contractile sheaths could be visualized. The individual T6SSs were mainly assembled at the site of contact with neighboring bacterial cells, whereby periplasmic proteins as well as the outer membrane protein OmpA mediated this localization (Lin et al., 2022).

SIM was also used to show distributions of the type 9 secretion system components GldL, GldM, GldK and GldN in *Flavobacterium johnsoniae*. All of these proteins seem to be distributed in foci along the bacterial circumference. GldK and GldN, which are part of the GldKN complex, showed in average less foci per cell than GldL and GldM, suggesting two subpopulations of GldLM complexes, one free and one associated with

GldKN rings (Vincent et al., 2022).

In a comprehensive super-resolution microscopy study of a T3SS, various T3SS components in *Salmonella Typhimurium* were labeled with fluorescent antibodies or the photoswitchable fluorophore mEos 3.2 and visualized with 2D and 3D SMLM (Zhang et al., 2017). Thereby, subcellular distributions and rough numbers of needle complexes, sorting platform components, tip complex and an effector could be determined. Needle complexes including export apparatus were almost exclusively located at the bacterial plasma membrane, whereas a considerable fraction of sorting platform components was also in the cytoplasm, suggesting that sorting platforms are transiently and dynamically associated with the needle complexes (Prindle et al., 2022) (Diepold et al., 2017). The relative stoichiometries of components of the sorting platform and export apparatus could be determined, confirming previous observations using other techniques (Diepold et al., 2015, Zilkenat et al., 2016, Diepold et al., 2017). Further, due to the estimated resolution of 35nm of the microscopic technique, the needle complex protein PrgH (unified nomenclature: SctD) and the tip complex protein SipD (unified nomenclature: SctA) could be visualized at a distance of 100 nm in individual injectisomes (Fig. 1A). It was also found that needle complexes are essential for the assembly of sorting platforms and that the effector SopB is mainly found in clusters in the cytoplasm and this does not depend on the parallel presence of needle complexes or sorting platforms (Zhang et al., 2017).

STED microscopy and SIM were used to visualize the *Yersinia enterocolitica* T3SS pore complex proteins YopB and YopD (unified nomenclature: SctE and SctB, respectively) in infected host cells. Per bacterium 30 what appeared to be single translocation pores at the tip of injectisome needles formed upon host cell contact. The two pore proteins YopB and YopD on one side and the needle complex/basal body protein component YscD (unified nomenclature: SctD) on the other side of single injectisomes could be resolved at a mean distance of 109 nm. Further, 3D-STED microscopy allowed to localize YopB in translocation pores which formed in a peculiar pre-vacuolar compartment in the infected cells (Nauth et al., 2018). To minimize the label error for MINFLUX nanoscopy, an ALFA-tag was introduced into YopD's extracellular domain (giving rise to YopD-ALFA). It was demonstrated that the ALFA-tag did not compromise the central functions of YopD during protein translocation by the *Y. enterocolitica* T3SS (Rudolph et al., 2022). MINFLUX nanoscopy allowed to visualize single YopD-ALFA molecules bound by fluorescent nanobodies in *Yersinia* translocation pores. The localization precision was ~ 5 nm and thus the size of the pore could be determined to be ~ 18 nm. Further, clusters consisting of 12 molecules of sorting platform protein YscL (unified nomenclature: SctL) fused with a HaloTag were recorded by 2D and 3D MINFLUX microscopy. With an isotropic localization precision of ~ 5 nm, these experiments could reproduce the size of the YscL structure determined by Cryo ET to be ~ 16 nm in diameter (Carsten et al., 2022) (Berger et al., 2021). 3D MINFLUX experiments performed in whole bacteria showed that the YscL complexes localized almost exclusively at the plasma membrane and at very low distances to each other (down to ~ 10 nm apart) (Carsten et al., 2022).

SMT and SMLM in live *Yersinia enterocolitica* revealed distinct diffusive states of the eYFP, eGFP and PAmCherry labelled sorting platform components YscQ, YscL and YscN (unified nomenclature: SctQ, SctL and SctN) and suggested that they form distinct cytosolic complexes before binding to the needle complex (Rocha et al., 2018, Prindle et al., 2022, Diepold et al., 2015). SMT of eGFP labelled YscD (unified nomenclature: SctD) showed partial disassembly of the T3SS basal body component at low external pH (Wimmi et al., 2021).

PALM was used to show that the *Salmonella* pathogenicity island-2 (SPI-2) signaling proteins SsrA/B labeled with PAmCherry were induced under low pH conditions. Furthermore, SMT identified pH-dependent DNA binding of SsrB (Liew et al., 2019).

Recently Halo-tagged *S. enterica* effectors PipB2, SseF, SseJ and SifA were visualized using SMT and SMLM. A bidirectional motility along tubular membrane structures of SseF, SifA and PipB2 was revealed providing novel and comprehensive information about the mobility of *Salmonella* SPI-2 effectors. Co-motion tracking analysis showed identical movement patterns of PipB2 together with the GFP labelled host protein LAMP1 (Goser et al., 2023).

Perspectives

SRM and SMT are rapidly developing technologies that are expected to allow major advances in understanding bacterial cell biology in the future. 1) Live-STED microscopy has the potential to image fluorescently labeled molecules during complex bacterial processes with up to 5-times better resolution than conventional live cell microscopy (Stockhammer, 2020). 2) New developments and optimizations of fluorescent probes (e.g., concerning on-/off-switching properties, brightness), especially for MINFLUX nanoscopy, will increase the versatility and flexibility of the method, e.g., in multicolor and live imaging as well as SMT (Remmel et al., 2023). 3) Combining MINFLUX nanoscopy with a PAINT-labeling approach may enable parallel imaging of three or more molecules of interest (Ostersehl et al., 2022). 4) Advanced labeling approaches of molecules may also open up unforeseen methodological options. E.g., the internal ALFA tag in *Y. enterocolitica* YopD (see above) can be bound by fluorescent nanobodies added extracellularly during a bacterial cell infection, allowing the kinetics of T3SS pore assembly and disassembly to be visualized in living bacteria and host cells (Rudolph et al., 2022).

Finally, the ability of MINFLUX tracking to directly observe the movements of single molecules promises new insights into the structure-function relationship of complex molecular processes in living bacterial and host cells. Particularly the spatiotemporal resolution that could be achieved with this technology was something that could not have been dreamed of not so long ago (Deguchi et al., 2023, Wolff et al., 2023).

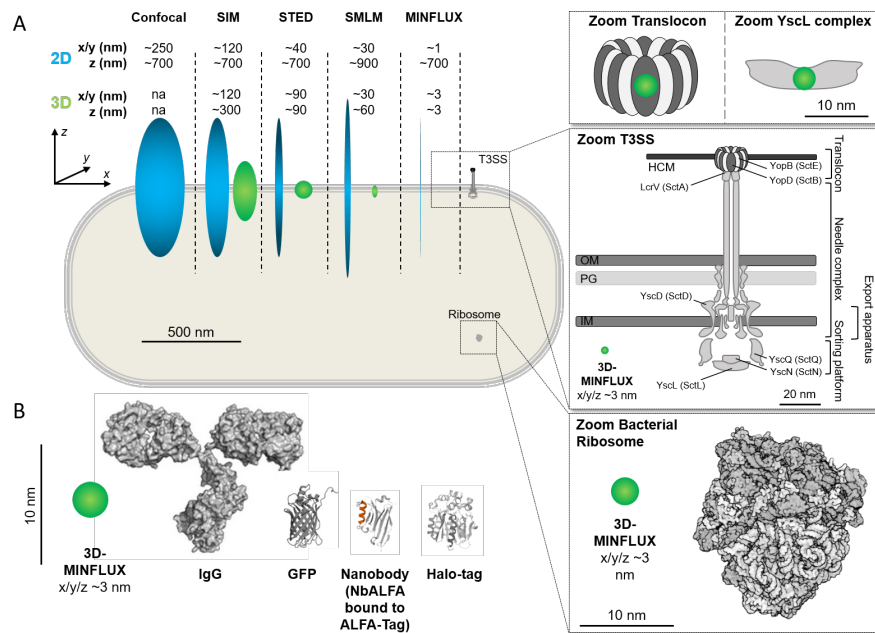


Figure 1: Approximate resolution of different fluorescence microscopy methods using the example of a Gram-negative bacterial cell with a ribosome and a type 3 secretion system (T3SS). (A) Schematic true-scale representation of a Gram-negative rod-shaped bacterium (1 μm width, 2.5 μm length) carrying a T3SS (~40 nm width, ~150 nm length) and a ribosome (~20 nm diameter). The ellipsoids represent the approximate resolution in x , y and z for confocal microscopy, structured illumination microscopy (SIM), stimulated emission depletion (STED) nanoscopy, single molecule localization microscopy (SMLM) and minimal photon flux (MINFLUX) nanoscopy. Approximate resolution values in 2D (blue) and 3D (green) mode of the indicated microscopy methods are shown. The T3SS, its translocon and YscL complex and the 3D-MINFLUX ellipsoid are shown enlarged in the insets. IM, inner membrane; PG, peptidoglycan layer; OM, outer membrane; HCM, host cell membrane. (B) True-scale representation of various molecules used for fluorescent labelling of target structures in relation to the 3D-MINFLUX nanoscopy resolution.

Structures were obtained from the Protein Data Bank (PDB): 1igt (IgG), 5dty (green fluorescent protein), 6i2g (NbALFA bound to ALFA-tag), 6y7a (Halo-tag) and 7k00 (bacterial ribosome).

Table 1: Selected super resolution microscopy studies in bacteria

Technique(s)	Biological target	Labelling method	Live/fixed	Organism	Reference
cell wall 3D STORM (dual-color imaging)	cell wall Membrane N- acetylglucosamine A enterotoxin B	cell wall nile red WGA (AF647) Indirect immunofluores- cence staining (AF647) Indirect immunofluores- cence staining (AF647)	cell wall fixed	cell wall <i>Staphylococcus aureus</i>	cell wall 10.1186/s12915- 022-01472-3
dSTORM	peptidoglycan	azido-D-Ala- D-Ala probe linked to AF647	fixed	<i>Streptococcus pneumoniae</i>	10.1016/j.xpro.2021.1010
dSTORM/ 3D-SIM	penicillin- binding proteins glycan strands	CephCy5 azide N-acetylmuramic acid (AzNAM)	fixed	<i>Staphylococcus aureus</i>	10.1021/acschembio.2c00
STED/SIM	peptidoglycan	Fluorescein/OregonGreen488/ TAMARA- labelled d-amino acids	fixed	<i>Staphylococcus aureus Streptococcus mutans Bacillus subtilis Escherichia coli Zymomonas mobilis</i>	10.1099/mic.0.000996
3D-SIM	Z-ring (SepF and FtsZ)	indirect immunofluo- rescence staining (AF555 and AF488)	fixed	<i>Methanobrevibacter smithii</i>	10.1038/s41467- 021-23099-8
3D-SIM	bactofilin (CcmA)	HaloTag (JF549)	fixed	<i>Helicobacter pylori</i>	10.7554/eLife.80111
SIM	teixobactin	fluorescent teixobactin analogues (fluorescein, Cy3 and Cy5)	fixed	<i>Bacillus subtilis</i>	10.1039/d2sc01388f
DNA PALM (SMT)	DNA DNA methyl- transferase (DnmA)	DNA PAmCherry	DNA live	DNA <i>Bacillus subtilis</i>	DNA 10.1128/mbio.03185- 22

Technique(s)	Biological target	Labelling method	Live/fixed	Organism	Reference
PALM (SMT)	translesion synthesis polymerases (Pol IV) single-stranded DNA-binding protein (SSB)	PAmCherry, mYPet	live	<i>Escherichia coli</i>	10.1073/pnas.220887511
PALM (imaging/ SMT) PAINT	two-component system SsrB, SsrA membranes	PAmCherry Nile red	fixed/live	<i>Salmonella enterica</i>	10.7554/eLife.45311
PALM (imaging/ SMT) 3D-SIM	RNA polymerase Nucleoid	PAmCherry HU-mCherry	fixed/live	<i>Escherichia coli</i>	10.1073/pnas.150759211
PALM (imaging/ SMT) SIM	DNA polymerase I ligase extracellular polysaccharides eDNA	PamCherry fluorescein isothiocyanate-labeled concanavalin A propidium iodide	fixed/live	<i>Escherichia coli</i>	10.1073/pnas.130180411
secretion systems 2D/3D-MINFLUX/ STORM/ STED	secretion systems T3SS translocon (YopD) T3SS basal body (YscD)	secretion systems ALFA-Tag/NbALFA based labelling (AbberiorSTAR635P, AF647) Halo-Tag (AF647)	secretion systems fixed	secretion systems <i>Yersinia enterocolitica</i>	secretion systems 10.1088/2050-6120/aca880
PALM (SMT)	T3SS basal body (YscD)	PAmCherry	live	<i>Yersinia enterocolitica</i>	10.1038/s41467-021-21863-4
PALM (imaging/ SMT)	SecYEG translocon ATPase (SecA)	Ypet/mEos3.2	fixed/ live	<i>Escherichia coli</i>	10.1038/s41598-021-81081-2
2D/3D-PALM (dual-color imaging)	T3SS PrgH, SpaO, OrgA, OrgB, InvC, InvI, InvA SipD	mEos3.2 indirect immunofluorescence staining (flag-tag, AF647)	fixed	<i>Salmonella enterica</i>	10.1073/pnas.170582311
dSTORM (dual-color imaging/ SMT)	flagellar basal body complex (FliN) T1SS ATPase subunit (SiiF) T1SS Secretin (SiiC) T3SS export apparatus (SpaS) T3SS ATPase (InvC)	Halo (TMR, Atto6) SNAP (TMR-Star)	fixed/ live	<i>Salmonella enterica</i>	10.1038/srep31601

Technique(s)	Biological target	Labelling method	Live/fixed	Organism	Reference
2D/3D-STED (dual-color imaging)/ SIM	T3SS translocon (YopB, YopD, LcrV) T3SS basal body YscD	indirect immunofluorescence staining (AbberiorSTARRed and AF594) GFP	fixed	<i>Yersinia enterocolitica</i>	10.1371/journal.ppat.100
2D/3D-STED	T3SS translocon (YopD)	ALFA-Tag/NbALFA based labelling (AF647, AbberiorSTAR635P)	fixed	<i>Yersinia enterocolitica</i>	10.1371/journal.ppat.100
2D/3D-SIM	T6SS proteins (TssB, TssA) Type six secretion dynamic localization protein A (TslA)	sfGFP/ <i>mCherry2</i> / <i>mNeonGreen</i> indirect immunofluorescence staining (AF594)	fixed	<i>Acinetobacter spp.</i> <i>Burkholderia thailandensis</i>	10.15252/embj.20211083
SIM	T9SS components (GldL and GldM) Adhesin (SprB)	indirect immunofluorescence staining (AF488, AF561)	fixed	<i>Flavobacterium johnsoniae</i>	10.1371/journal.pbio.300
SIM	T4SS protein (VirB6a)	sfGFP	fixed	<i>Agrobacterium tumefaciens</i>	10.1074/jbc.RA118.0027
adhesins, virulence factors DNA-PAINT	adhesins, virulence factors fibronectin binding proteins (FnBPA and FnBPB)	adhesins, virulence factors Fn conjugated to a DNA-PAINT docking sequence, Cy3B-labeled complementary imager strands	adhesins, virulence factors fixed	adhesins, virulence factors <i>Staphylococcus aureus</i>	adhesins, virulence factors 10.1021/acsnano.2c00630
PAINT/dSTORM (dual-color imaging)	listeriolysin S membrane	Direct immunofluorescence staining (HA-tag, AF647) Nile red	fixed	<i>Listeria monocytogenes</i>	10.1073/pnas.210815511
PALM, dSTORM; dSTORM/PALM (dual-color imaging)	F-type ATPase (F ₁ -like-X ₀) protease (MIP ₀₅₈₂)	mEos3.2 indirect immunofluorescence staining (HA-tag, AF647)	fixed	<i>Mycoplasma spp.</i>	10.1128/spectrum.00645-22

Technique(s)	Biological target	Labelling method	Live/fixed	Organism	Reference
SIM	hemolysin A (HlyA)	eGFP/ Indirect immunofluorescence staining (Cy3 or AbberiorStar635P)	fixed	<i>Escherichia coli</i>	10.1128/AEM.01896-21

References

- BALZAROTTI, F., EILERS, Y., GWOSCH, K. C., GYNNA, A. H., WESTPHAL, V., STEFANI, F. D., ELF, J. & HELL, S. W. 2017. Nanometer resolution imaging and tracking of fluorescent molecules with minimal photon fluxes. *Science*, 355, 606-612.
- BANAZ, N., MAKELA, J. & UPHOFF, S. 2019. Choosing the right label for single-molecule tracking in live bacteria: side-by-side comparison of photoactivatable fluorescent protein and Halo tag dyes. *J Phys D Appl Phys*, 52, 064002.
- BARLAG, B., BEUTEL, O., JANNING, D., CZARNIAK, F., RICHTER, C. P., KOMMNICK, C., GOSER, V., KURRE, R., FABIANI, F., ERHARDT, M., PIEHLER, J. & HENSEL, M. 2016. Single molecule super-resolution imaging of proteins in living *Salmonella enterica* using self-labelling enzymes. *Sci Rep*, 6, 31601.
- BEER, T., HANSCH, S., PFEFFER, K., SMITS, S. H. J., WEIDTKAMP-PETERS, S. & SCHMITT, L. 2022. Quantification and Surface Localization of the Hemolysin A Type I Secretion System at the Endogenous Level and under Conditions of Overexpression. *Appl Environ Microbiol*, 88, e0189621.
- BERGER, C., RAVELLI, R. B. G., LOPEZ-IGLESIAS, C., KUDRYASHEV, M., DIEPOLD, A. & PETERS, P. J. 2021. Structure of the *Yersinia* injectisome in intracellular host cell phagosomes revealed by cryo FIB electron tomography. *J Struct Biol*, 213, 107701.
- BETZIG, E., PATTERSON, G. H., SOUGRAT, R., LINDWASSER, O. W., OLENYCH, S., BONIFACINO, J. S., DAVIDSON, M. W., LIPPINCOTT-SCHWARTZ, J. & HESS, H. F. 2006. Imaging intracellular fluorescent proteins at nanometer resolution. *Science*, 313, 1642-5.
- BOLOGNESI, B. & LEHNER, B. 2018. Reaching the limit. *Elife*, 7.
- BUTTNER, M., LAGERHOLM, C. B., WAITHE, D., GALIANI, S., SCHLIEBS, W., ERDMANN, R., EGGELING, C. & REGLINSKI, K. 2021. Challenges of Using Expansion Microscopy for Super-resolved Imaging of Cellular Organelles. *Chembiochem*, 22, 686-693.
- CARSTEN, A., RUDOLPH, M., WEIHS, T., SCHMIDT, R., JANSEN, I., WURM, C. A., DIEPOLD, A., FAILLA, A. V., WOLTERS, M. & AEPFELBACHER, M. 2022. MINFLUX imaging of a bacterial molecular machine at nanometer resolution. *Methods Appl Fluoresc*, 11.
- CASSARO, C. J. & UPHOFF, S. 2022. Super-Resolution Microscopy and Tracking of DNA-Binding Proteins in Bacterial Cells. *Methods Mol Biol*, 2476, 191-208.
- CHEN, F., TILLBERG, P. W. & BOYDEN, E. S. 2015. Optical imaging. Expansion microscopy. *Science*, 347, 543-8.
- DEANE, J. E., ROVERSI, P., CORDES, F. S., JOHNSON, S., KENJALE, R., DANIELL, S., BOOY, F., PICKING, W. D., PICKING, W. L., BLOCKER, A. J. & LEA, S. M. 2006. Molecular model of a type III secretion system needle: Implications for host-cell sensing. *Proc Natl Acad Sci U S A*, 103, 12529-33.
- DEGUCHI, T., IWANSKI, M. K., SCHENTARRA, E. M., HEIDEBRECHT, C., SCHMIDT, L., HECK, J., WEIHS, T., SCHNORRENBERG, S., HOESS, P., LIU, S., CHEVYREVA, V., NOH, K. M., KAPITEIN,

- L. C. & RIES, J. 2023. Direct observation of motor protein stepping in living cells using MINFLUX. *Science*, 379, 1010-1015.
- DIEPOLD, A., KUDRYASHEV, M., DELALEZ, N. J., BERRY, R. M. & ARMITAGE, J. P. 2015. Composition, formation, and regulation of the cytosolic c-ring, a dynamic component of the type III secretion injectisome. *PLoS Biol*, 13, e1002039.
- DIEPOLD, A., SEZGIN, E., HUSEYIN, M., MORTIMER, T., EGGELING, C. & ARMITAGE, J. P. 2017. A dynamic and adaptive network of cytosolic interactions governs protein export by the T3SS injectisome. *Nat Commun*, 8, 15940.
- FERNANDEZ, N. L., CHEN, Z., FULLER, D. E. H., VAN GIJTENBEEK, L. A., NYE, T. M., BITEEN, J. S. & SIMMONS, L. A. 2023. DNA Methylation and RNA-DNA Hybrids Regulate the Single-Molecule Localization of a DNA Methyltransferase on the Bacterial Nucleoid. *mBio*, 14,e0318522.
- FILLOUX, A. 2022. Bacterial protein secretion systems: Game of types. *Microbiology (Reading)*, 168.
- FRUH, S. M., MATTI, U., SPYCHER, P. R., RUBINI, M., LICKERT, S., SCHLICHTHAERLE, T., JUNG-MANN, R., VOGEL, V., RIES, J. & SCHOEN, I. 2021. Site-Specifically-Labeled Antibodies for Super-Resolution Microscopy Reveal In Situ Linkage Errors. *ACS Nano*, 15,12161-12170.
- GALAN, J. E. 2009. Common themes in the design and function of bacterial effectors. *Cell Host Microbe*, 5, 571-9.
- GOSER, V., KOMMNICK, C., LISS, V. & HENSEL, M. 2019. Self-Labeling Enzyme Tags for Analyses of Translocation of Type III Secretion System Effector Proteins. *mBio*, 10.
- GOSER, V., SANDER, N., SCHULTE, M., SCHARTE, F., FRANZKOCH, R., LISS, V., PSATHAKI, O. E. & HENSEL, M. 2023. Single molecule analyses reveal dynamics of Salmonella translocated effector proteins in host cell endomembranes. *Nat Commun*, 14, 1240.
- GOTZ, R., KUNZ, T. C., FINK, J., SOLGER, F., SCHLEGEL, J., SEIBEL, J., KOZJAK-PAVLOVIC, V., RUDEL, T. & SAUER, M. 2020. Nanoscale imaging of bacterial infections by sphingolipid expansion microscopy. *Nat Commun*, 11, 6173.
- GUSTAFSSON, M. G. 2000. Surpassing the lateral resolution limit by a factor of two using structured illumination microscopy. *J Microsc*, 198, 82-7.
- GUSTAFSSON, M. G., SHAO, L., CARLTON, P. M., WANG, C. J., GOLUBOVSKAYA, I. N., CANDE, W. Z., AGARD, D. A. & SEDAT, J. W. 2008. Three-dimensional resolution doubling in wide-field fluorescence microscopy by structured illumination. *Biophys J*, 94,4957-70.
- HELL, S. W. & WICHMANN, J. 1994. Breaking the diffraction resolution limit by stimulated emission: stimulated-emission-depletion fluorescence microscopy. *Opt Lett*, 19, 780-2.
- HU, J., WORRALL, L. J., HONG, C., VUCKOVIC, M., ATKINSON, C. E., CAVENEY, N., YU, Z. & STRYNADKA, N. C. J. 2018. Cryo-EM analysis of the T3S injectisome reveals the structure of the needle and open secretin. *Nat Commun*, 9, 3840.
- JENKINS, J., WORRALL, L. J. & STRYNADKA, N. C. J. 2022. Recent structural advances towards understanding of the bacterial type III secretion injectisome. *Trends Biochem Sci*, 47, 795-809.
- JEONG, D., KIM, M. J., PARK, Y., CHUNG, J., KWEON, H. S., KANG, N. G., HWANG, S. J., YOUN, S. H., HWANG, B. K. & KIM, D. 2022. Visualizing extracellular vesicle biogenesis in gram-positive bacteria using super-resolution microscopy. *BMC Biol*, 20, 270.
- KHATEB, H., SORENSEN, R. S., CRAMER, K., EKLUND, A. S., KJEMS, J., MEYER, R. L., JUNG-MANN, R. & SUTHERLAND, D. S. 2022. The Role of Nanoscale Distribution of Fibronectin in the Adhesion of Staphylococcus aureus Studied by Protein Patterning and DNA-PAINT. *ACS Nano*, 16, 10392-10403.

- KLAR, T. A. & HELL, S. W. 1999. Subdiffraction resolution in far-field fluorescence microscopy. *Opt Lett*, 24, 954-6.
- KUNZ, T. C., RUHLING, M., MOLDOVAN, A., PAPROTKA, K., KOZJAK-PAVLOVIC, V., RUDEL, T. & FRAUNHOLZ, M. 2021. The Expandables: Cracking the Staphylococcal Cell Wall for Expansion Microscopy. *Front Cell Infect Microbiol*, 11, 644750.
- LARA-TEJERO, M., KATO, J., WAGNER, S., LIU, X. & GALAN, J. E. 2011. A sorting platform determines the order of protein secretion in bacterial type III systems. *Science*, 331, 1188-91.
- LE, N. H., PINEDO, V., LOPEZ, J., CAVA, F. & FELDMAN, M. F. 2021. Killing of Gram-negative and Gram-positive bacteria by a bifunctional cell wall-targeting T6SS effector. *Proc Natl Acad Sci U S A*, 118.
- LIEW, A. T. F., FOO, Y. H., GAO, Y., ZANGOUI, P., SINGH, M. K., GULVADY, R. & KENNEY, L. J. 2019. Single cell, super-resolution imaging reveals an acid pH-dependent conformational switch in SsrB regulates SPI-2. *Elife*, 8.
- LIN, L., CAPOZZOLI, R., FERRAND, A., PLUM, M., VETTIGER, A. & BASLER, M. 2022. Subcellular localization of Type VI secretion system assembly in response to cell-cell contact. *EMBO J*, 41, e108595.
- LISS, V., BARLAG, B., NIETSCHKE, M. & HENSEL, M. 2015. Self-labelling enzymes as universal tags for fluorescence microscopy, super-resolution microscopy and electron microscopy. *Sci Rep*, 5, 17740.
- LIU, S., HOESS, P. & RIES, J. 2022. Super-Resolution Microscopy for Structural Cell Biology. *Annu Rev Biophys*, 51, 301-326.
- LUND, V. A., GANGOTRA, H., ZHAO, Z., SUTTON, J. A. F., WACNIK, K., DEMEESTER, K., LIANG, H., SANTIAGO, C., LEIMKUEHLER GRIMES, C., JONES, S. & FOSTER, S. J. 2022. Coupling Novel Probes with Molecular Localization Microscopy Reveals Cell Wall Homeostatic Mechanisms in *Staphylococcus aureus*. *ACS Chem Biol*, 17, 3298-3305.
- LUNELLI, M., KAMPRAD, A., BURGER, J., MIELKE, T., SPAHN, C. M. T. & KOLBE, M. 2020. Cryo-EM structure of the *Shigella* type III needle complex. *PLoS Pathog*, 16, e1008263.
- MARLOVITS, T. C., KUBORI, T., SUKHAN, A., THOMAS, D. R., GALAN, J. E. & UNGER, V. M. 2004. Structural insights into the assembly of the type III secretion needle complex. *Science*, 306, 1040-2.
- MARY, C., FOUILLEN, A., BESSETTE, B., NANJI, A. & BARON, C. 2018. Interaction via the N terminus of the type IV secretion system (T4SS) protein VirB6 with VirB10 is required for VirB2 and VirB5 incorporation into T-pili and for T4SS function. *J Biol Chem*, 293,13415-13426.
- MEZA-TORRES, J., LELEK, M., QUEREDA, J. J., SACHSE, M., MANINA, G., ERSHOV, D., TINEVEZ, J. Y., RADOSHEVICH, L., MAUDET, C., CHAZE, T., GIAI GIANETTO, Q., MATONDO, M., LECUIT, M., MARTIN-VERSTRAETE, I., ZIMMER, C., BIERNE, H., DUSSURGET, O., COSSART, P. & PIZARRO-CERDA, J. 2021. Listeriolysin S: A bacteriocin from *Listeria monocytogenes* that induces membrane permeabilization in a contact-dependent manner. *Proc Natl Acad Sci U S A*, 118.
- MIHAILA, T. S., BATE, C., OSTERSEHLT, L. M., PAPE, J. K., KELLER-FINDEISEN, J., SAHL, S. J. & HELL, S. W. 2022. Enhanced incorporation of subnanometer tags into cellular proteins for fluorescence nanoscopy via optimized genetic code expansion. *Proc Natl Acad Sci U S A*, 119, e2201861119.
- MILETIC, S., FAHRENKAMP, D., GOESSWEINER-MOHR, N., WALD, J., PANTEL, M., VESPER, O., KOTOV, V. & MARLOVITS, T. C. 2021. Substrate-engaged type III secretion system structures reveal gating mechanism for unfolded protein translocation. *Nat Commun*, 12, 1546.
- MORRIS, M. A., VALLMITJANA, A., GREIN, F., SCHNEIDER, T., ARTS, M., JONES, C. R., NGUYEN, B. T., HASHEMIAN, M. H., MALEK, M., GRATTON, E. & NOWICK, J. S. 2022. Visualizing the mode of action and supramolecular assembly of teixobactin analogues in *Bacillus subtilis*. *Chem Sci*,13, 7747-7754.

- NAUTH, T., HUSCHKA, F., SCHWEIZER, M., BOSSE, J. B., DIEPOLD, A., FAILLA, A. V., STEFFEN, A., STRADAL, T. E. B., WOLTERS, M. & AEPFELBACHER, M. 2018. Visualization of translocons in Yersinia type III protein secretion machines during host cell infection. *PLoS Pathog*, 14, e1007527.
- OSTERSEHLT, L. M., JANS, D. C., WITTEK, A., KELLER-FINDEISEN, J., INAMDAR, K., SAHL, S. J., HELL, S. W. & JAKOBS, S. 2022. DNA-PAINT MINFLUX nanoscopy. *Nat Methods*, 19, 1072-1075.
- PENDE, N., SOGUES, A., MEGRIAN, D., SARTORI-RUPP, A., ENGLAND, P., PALABIKYAN, H., RITTMANN, S. K. R., GRANA, M., WEHENKEL, A. M., ALZARI, P. M. & GRIBALDO, S. 2021. SepF is the FtsZ anchor in archaea, with features of an ancestral cell division system. *Nat Commun*, 12, 3214.
- PRINDLE, J. R., WANG, Y., ROCHA, J. M., DIEPOLD, A. & GAHLMANN, A. 2022. Distinct Cytosolic Complexes Containing the Type III Secretion System ATPase Resolved by Three-Dimensional Single-Molecule Tracking in Live Yersinia enterocolitica. *Microbiol Spectr*, e0174422.
- REMMEL, M., SCHEIDERER, L., BUTKEVICH, A. N., BOSSI, M. L. & HELL, S. W. 2023. Accelerated MINFLUX Nanoscopy, through Spontaneously Fast-Blinking Fluorophores. *Small*, 19, e2206026.
- RIDEAU, F., VILLA, A., BELZANNE, P., VERDIER, E., HOSY, E. & ARFI, Y. 2022. Imaging Minimal Bacteria at the Nanoscale: a Reliable and Versatile Process to Perform Single-Molecule Localization Microscopy in Mycoplasmas. *Microbiol Spectr*, 10, e0064522.
- RIES, J., KAPLAN, C., PLATONOVA, E., EGHLIDI, H. & EWERS, H. 2012. A simple, versatile method for GFP-based super-resolution microscopy via nanobodies. *Nat Methods*, 9, 582-4.
- ROCHA, J. M., RICHARDSON, C. J., ZHANG, M., DARCH, C. M., CAI, E., DIEPOLD, A. & GAHLMANN, A. 2018. Single-molecule tracking in live Yersinia enterocolitica reveals distinct cytosolic complexes of injectisome subunits. *Integr Biol (Camb)*, 10, 502-515.
- RUDOLPH, M., CARSTEN, A., KULNIK, S., AEPFELBACHER, M. & WOLTERS, M. 2022. Live imaging of Yersinia translocon formation and immune recognition in host cells. *PLoS Pathog*, 18, e1010251.
- RUST, M. J., BATES, M. & ZHUANG, X. 2006. Sub-diffraction-limit imaging by stochastic optical reconstruction microscopy (STORM). *Nat Methods*, 3, 793-5.
- SAHL, S. J., HELL, S. W. & JAKOBS, S. 2017. Fluorescence nanoscopy in cell biology. *Nat Rev Mol Cell Biol*, 18, 685-701.
- SCHMIDT, R., WEIHS, T., WURM, C. A., JANSEN, I., REHMAN, J., SAHL, S. J. & HELL, S. W. 2021. MINFLUX nanometer-scale 3D imaging and microsecond-range tracking on a common fluorescence microscope. *Nat Commun*, 12, 1478.
- SCHNITZBAUER, J., STRAUSS, M. T., SCHLICHTHAERLE, T., SCHUEDER, F. & JUNGSMANN, R. 2017. Super-resolution microscopy with DNA-PAINT. *Nat Protoc*, 12, 1198-1228.
- SEINEN, A. B., SPAKMAN, D., VAN OIJEN, A. M. & DRIESSEN, A. J. M. 2021. Cellular dynamics of the SecA ATPase at the single molecule level. *Sci Rep*, 11, 1433.
- SICHEL, S. R., BRATTON, B. P. & SALAMA, N. R. 2022. Distinct regions of H. pylori's bactofilin CcmA regulate protein-protein interactions to control helical cell shape. *Elife*, 11.
- SINGH, M. K. & KENNEY, L. J. 2021. Super-resolution imaging of bacterial pathogens and visualization of their secreted effectors. *FEMS Microbiol Rev*, 45.
- SODERSTROM, B., RUDA, A., WIDMALM, G. & DALEY, D. O. 2020. An OregonGreen488-labelled d-amino acid for visualizing peptidoglycan by super-resolution STED nanoscopy. *Microbiology (Reading)*, 166, 1129-1135.
- STOCKHAMMER, A. 2020. Appreciating the small things in life: STED microscopy in living cells. *Journal of Physics D: Applied Physics*, 54.

- STRACY, M., LESTERLIN, C., GARZA DE LEON, F., UPHOFF, S., ZAWADZKI, P. & KAPANIDIS, A. N. 2015. Live-cell superresolution microscopy reveals the organization of RNA polymerase in the bacterial nucleoid. *Proc Natl Acad Sci U S A*, 112, E4390-9.
- TANK, R. K. G., LUND, V. A., KUMAR, S., TURNER, R. D., LAFAGE, L., PASQUINA LEMONCHE, L., BULLOUGH, P. A., CADBY, A., FOSTER, S. J. & HOBBS, J. K. 2021. Correlative Super-Resolution Optical and Atomic Force Microscopy Reveals Relationships Between Bacterial Cell Wall Architecture and Synthesis in *Bacillus subtilis*. *ACS Nano*, 15, 16011-16018.
- THRALL, E. S., PIATT, S. C., CHANG, S. & LOPARO, J. J. 2022. Replication stalling activates SSB for recruitment of DNA damage tolerance factors. *Proc Natl Acad Sci U S A*, 119, e2208875119.
- TROUVE, J., GLUSHONKOV, O. & MORLOT, C. 2021. Metabolic biorthogonal labeling and dSTORM imaging of peptidoglycan synthesis in *Streptococcus pneumoniae*. *STAR Protoc*, 2, 101006.
- TRUCKENBRODT, S., MAIDORN, M., CRZAN, D., WILDHAGEN, H., KABATAS, S. & RIZZOLI, S. O. 2018. X10 expansion microscopy enables 25-nm resolution on conventional microscopes. *EMBO Rep*, 19.
- UPHOFF, S., REYES-LAMOTHE, R., GARZA DE LEON, F., SHERRATT, D. J. & KAPANIDIS, A. N. 2013. Single-molecule DNA repair in live bacteria. *Proc Natl Acad Sci U S A*, 110, 8063-8.
- VEENENDAAL, A. K., HODGKINSON, J. L., SCHWARZER, L., STABAT, D., ZENK, S. F. & BLOCKER, A. J. 2007. The type III secretion system needle tip complex mediates host cell sensing and translocon insertion. *Mol Microbiol*, 63, 1719-30.
- VINCENT, M. S., COMAS HERVADA, C., SEBBAN-KREUZER, C., LE GUENNO, H., CHABALIER, M., KOSTA, A., GUERLESQUIN, F., MIGNOT, T., MCBRIDE, M. J., CASCALES, E. & DOAN, T. 2022. Dynamic proton-dependent motors power type IX secretion and gliding motility in *Flavobacterium*. *PLoS Biol*, 20, e3001443.
- WAGNER, S., GRIN, I., MALMSHEIMER, S., SINGH, N., TORRES-VARGAS, C. E. & WESTERHAUSEN, S. 2018. Bacterial type III secretion systems: a complex device for the delivery of bacterial effector proteins into eukaryotic host cells. *FEMS Microbiol Lett*, 365.
- WANG, Y., FU, M., WU, B., HUANG, M., MA, T., ZANG, H., JIANG, H., ZHANG, Y. & LI, C. 2022. Insight into biofilm-forming patterns: biofilm-forming conditions and dynamic changes in extracellular polymer substances. *Environ Sci Pollut Res Int*, 29, 89542-89556.
- WIMMI, S., BALINOVIC, A., JECKEL, H., SELINGER, L., LAMPAKI, D., EISEMANN, E., MEUSKENS, I., LINKE, D., DRESCHER, K., ENDESFELDER, U. & DIEPOLD, A. 2021. Dynamic relocalization of cytosolic type III secretion system components prevents premature protein secretion at low external pH. *Nat Commun*, 12, 1625.
- WOLFF, J. O., SCHEIDERER, L., ENGELHARDT, T., ENGELHARDT, J., MATTHIAS, J. & HELL, S. W. 2023. MINFLUX dissects the unimpeded walking of kinesin-1. *Science*, 379, 1004-1010.
- WORRALL, L. J., HONG, C., VUCKOVIC, M., DENG, W., BERGERON, J. R. C., MAJEWSKI, D. D., HUANG, R. K., SPRETER, T., FINLAY, B. B., YU, Z. & STRYNADKA, N. C. J. 2016. Near-atomic-resolution cryo-EM analysis of the *Salmonella* T3S injectisome basal body. *Nature*, 540, 597-601.
- ZHANG, Y., LARA-TEJERO, M., BEWERSDORF, J. & GALAN, J. E. 2017. Visualization and characterization of individual type III protein secretion machines in live bacteria. *Proc Natl Acad Sci U S A*, 114, 6098-6103.
- ZILKENAT, S., FRANZ-WACHTEL, M., STIERHOF, Y. D., GALAN, J. E., MACEK, B. & WAGNER, S. 2016. Determination of the Stoichiometry of the Complete Bacterial Type III Secretion Needle Complex Using a Combined Quantitative Proteomic Approach. *Mol Cell Proteomics*, 15, 1598-609.

Acknowledgements:

We thank Jost Enninga for helpful discussions and Antonio Virgilio Failla for critical reading of the manuscript. The selected papers on SRM/SMT and their applications in bacteria that we mention and cite in this article do not claim to be complete. We apologize to all colleagues whose papers we have not cited here due to space limitations or because we simply did not discover them during our extensive literature searches.

Funding:

This study was supported by a grant from the Joachim Herz Foundation to Alexander Carsten and by the DFG-funded RTG 2771 Humans and Microbes. Acquisition of the MINFLUX microscope was made possible through funding from the European Regional Development Fund (ERDF) under the Operational Programme Hamburg ERDF 2014-2020, REACT-EU, awarded by the Hamburgische Investitions- und Förderbank (grant number 51164232).

Conflict of interest:

The authors declare no conflict of interest.